JOURNAL OF AGRICULTURAL AND FOOD CHEMISTRY

Monitoring the Effects of Storage in Caviar from Farmed *Acipenser transmontanus* Using Chemical, SEM, and NMR Methods†

MARISTELLA GUSSONI,‡ FULVIA GRECO,§ ALESSANDRA VEZZOLI,# MARIA ANTONIETTA PALEARI,⊥ VITTORIO MARIA MORETTI,⊥ GIUSEPPE BERETTA,⊥ FABIO CAPRINO,⊥ BARBARA LANZA,|| AND LUCIA ZETTA*,§

Dipartimento di Scienze e Tecnologie Biomediche, Università di Milano, Segrate (MI), I-20090 Italy; Lab. NMR, Istituto per lo Studio delle Macromolecole, CNR, Milano, I-20133 Italy; Istituto Bioimmagini and Fisiologia Molecolare, CNR, Milano, I-20133 Italy; Dipartimento di Scienze e Tecnologie Veterinarie per la Sicurezza Alimentare, Università di Milano, Milano, I-20133 Italy; and Istituto Sperimentale per la Elaiotecnica, Città S. Angelo (PE), I-65013 Italy

The effects of storage at 4 °C on the quantity and quality of chemical components in the caviar from farmed *Acipenser transmontanus* have been analyzed by SEM, chemical methods, and NMR and MRI techniques. Particular attention has been focused on the lipid components, the distribution and mobility of which were strongly affected by the storage time. MRI and relaxation data indicated that lipids are endowed with two different mobility regimes, one slow (short T_1) and one fast (long T_1), both lengthening with the storage time. Chemical analysis assessed a total fat content that remained practically unchanged and a constant fatty acid composition during the total storage time. The combination of the two methods allowed one (a) to suppose that a mechanism of lipid hydrolysis (faster in unsalted than in salted eggs) is still occurring during storage of caviar at 4 °C for up to ≈4 months and (b) to exclude that an intensive oxidative process is active in the same storage period.

KEYWORDS: Caviar; NMR; relaxation times; MRI; chemical analysis; SEM; fatty acids

INTRODUCTION

Lipids of food play a fundamental role in human nutrition, because of their essential fatty acid contents (*1*). The fatty acid composition of fish lipids is characterized by a richness in long-chain polyunsaturated fatty acids (PUFA), especially the n-3 ones. The importance of these fatty acids is well-known in human health, due to their role in cardiovascular disease prevention (*2*, *3*). Hen's egg yolk lipoproteins are important for lipid-mediated antimicrobial activity and for antioxidant effects that are able to prevent oxidation of unsaturated fatty acids. Such activity increases upon treatment with digestive enzymes, indicating that degradation might be required for the maximal levels of the active components to be released (*4*). It has been found that lipids and lipoproteins, as well as their components oleic and linolenic acids, when extracted from hen's egg yolk, exert antimicrobial effect against *Streptococcus* (*5*).

It is known that large size fish species (sturgeon included) need a short storage period after slaughtering to age the tissues and to acquire flavors (*6*−*8*). Nevertheless, during the storage, lipids show important quantity−quality modifications, especially of the fatty acids composition (*9*, *10*). The oxidation products of the unsaturated fatty acids contribute also to the flavor and color of meat (*11*, *12*). Therefore, chemical and biochemical modifications of lipids during storage influence the nutritional and sensory properties of fish. Nowadays, interest in the quality of fishery and aquaculture products has a big economic impact due to the high nutritional value and strong demand for authenticity.

In the present paper we put in evidence the effects of storage at 4 °C on the quantity and quality of lipid components in the caviar from farmed *Acipenser transmontanus.* To this aim, magnetic resonance imaging (MRI) and spectroscopic T_1 and T_2 proton relaxation techniques have been used to study structural properties and conservation state of salted caviar during storage for up to 120 days. For comparison, scanning electron microscopy (SEM) images were separately collected and thoroughly analyzed.

T_1 and T_2 relaxation parameters are related to proton mobility and, at the same time, water and lipid mobility are strictly associated with cell metabolism. With regard to food science, a variety of physical as well as nuclear magnetic resonance

† Dedicated to the memory of Professor Giorgio Bianchi.
‡ Dipartimento di Scienze e Tecnologie Biomediche, Università di Milano.
§ Istituto per lo Studio delle Macromolecole, CNR.
# Istituto Bioimmagini and Fisiologiz Molecolare, CNR.
⊥ Dipartimento di Scienze e Tecnologie Veterinarie per la Sicurezza Alimentare, Università di Milano.
|| Istituto Sperimentale per la Elaiotecnica.

10.1021/jf061286f CCC: $33.50
Published on Web 08/16/2006

(NMR) spectroscopic and imaging techniques, including NMR relaxometry (*13*), have been used to quantify food heterogeneity and to measure the microscopic distribution of water and lipid in the food matrix, distribution that might be altered during processing and storage.

Up to now, only a few SEM studies have been devoted to gaining insights into the histology and ultrastructure of white sturgeon oocytes (*14*) as well as into caviar species identification (*15*) and composition (*16*, *17*). To our knowledge, caviar has never been investigated by NMR or MRI.

MATERIALS AND METHODS

Materials. For NMR and SEM experiments and chemical analyses 15 caviar samples from farmed *A. transmontanus* were provided by Agroittica Lombarda (Calvisano, BS, Italy).

Among the numerous sturgeon species and hybrids, the white sturgeon *A. transmontanus*, native to the North American Pacific coast, is of particular importance in Italy. Not only is this species suited to intensive farming conditions, but also its flesh (both fresh and processed) is well appreciated by the consumer.

Caviar comes from sexually mature females of white sturgeon weighing ≈25−40 kg.

The ovaries are withdrawn from the opened abdominal cavity and delicately massaged to release the eggs, which then undergo a brief washing stage followed by dry salting with salt. At the end of salting the product has a salt concentration of 2.5−3% and is classified as "malossol" (lightly salted). The caviar "grains" are ≈3 mm in diameter and pale in color. Usually the yield of caviar is ≈10% of the body weight of the sturgeon. The caviar samples used in these experiments were all taken from the same animal, a 29 kg female of sturgeon *A. transmontanus*, packed in metal cans (50 g each), and stored at 4 °C until analysis.

Experiments were performed at the same time on unsalted (or raw) and salted oocytes, starting from the day of isolation (0) and after 30, 60, 90, and 120 days of storage. The mean weight of oocytes at 0 day was around 18 mg for unsalted and salted samples. The caviar samples were stored in hermetically closed commercial metal cans, 50 g each. During chemical and NMR experiments, boxes were kept in the refrigerator at 4 °C. Testing boxes were opened a few minutes before the beginning of the experimental session. NMR imaging and relaxation experiments were performed on different oocyte samples taken from the same box.

SEM Preparation. Fresh and NaCl-salted oocytes were fixed in 3% glutaraldehyde in 0.05 M cacodylate buffer (pH 7.2) for 12 h at 0−4 °C. Fixed eggs were cut with a razor blade across the equatorial diameter to allow observation of the internal structure and the envelope layers. The samples were washed with the same buffer and then postfixed in 1% osmium tetroxide in H_2O. The fixed tissues were dehydrated in ethanol series (10, 30, 50, 70, 90, 95, and 100%) and then transferred to acetone before drying in a critical point dryer (Balzers CPD 030) using liquid CO_2. The dry tissues were then mounted, fracture surface upward, onto aluminum stubs with double-stick tape and coated with gold (25 nm thick) in a sputter coater (Balzers SCD 050). Representative specimens were observed at 10−20 kV with a SEM Philips XL 20 equipped with Image Analysis System (AnalySIS 1.22) to obtain measurements of the different tissues.

^{1}H NMR Relaxation and MRI. Proton NMR T_1 and T_2 relaxation and MRI experiments were carried out on a 4.7 T Bruker AM WB spectrometer (Bruker, Karlsruhe, Germany) equipped with a probehead tuneable at the ^{1}H resonance frequency (200.13 MHz) and a gradient drive unit utilized for MRI experiments. Orthogonal field gradient coils, built into the probehead, were capable of achieving gradients up to 150 G/cm, with a trigger pulse of 5 μs for switching the gradients. Because in this configuration the instrument was not provided with a field frequency stabilization (lock channel), at the beginning of each experiment, the field frequency was set on the water proton resonance that resulted at ≈4.7 ppm downfield from the sodium 3-trimethylsilylpropionate (TSP) proton resonance, used as internal reference.

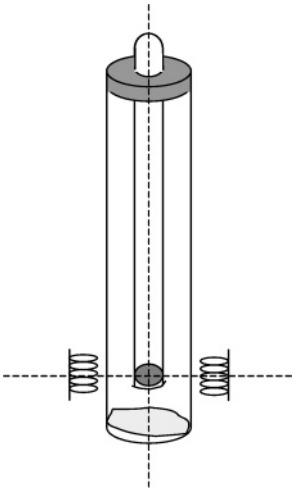

Figure 1. Single oocyte put at the open end of a 5-mm NMR tube and fixed with a riddled Parafilm. The 5-mm tube was coaxially hung, upside down, into a 10-mm NMR tube. The oocyte was centered inside the active coil region. A small amount of water was put into the bottom of the 10-mm tube to keep the sample wet.

Samples for NMR were prepared as indicated in **Figure 1**. A single oocyte was carefully put at the open end of a 5-mm NMR tube and fixed with a riddled Parafilm. The 5-mm tube was hung upside down, into a 10-mm NMR tube, where it was fixed with two plugs. A small amount of water was put into the bottom of the 10-mm tube to keep the sample wet. The tube system was inserted into the probe, centering the oocyte and taking water outside the active coil region.

All NMR experiments were carried out using a 10-mm insert. The proton 1D NMR spectrum, collected on the oocyte sample at the beginning of each experimental session, showed the water resonance (set at 4.7 ppm) only ascribable to the intracellular water protons and four well-resolved major resonances from methylene (2.65, 1.96, and 1.168 ppm) and methyl (0.815 ppm) lipid protons. The Gaussian selective pulse (1 ms) was centered on the lipid peak at 1.168 ppm, in order to perform chemical shift selective imaging and relaxation experiments on lipids.

MRI experiments were carried out employing phase/frequency encoding two-dimensional (2D) lipid selective spin−echo sequences standardly supplied by Bruker. All MRI experiments were performed during the same experimental session on both unsalted and salted samples, by using the same pulse sequences and adopting the same acquisition parameters. Transverse (*xy*) spin−echo images were acquired with 30 averages (NE), so obtaining each image in ≈1 h. For all images, acquisition parameters were as follows: 256 × 256 matrix; field of view (FOV) = 0.6 cm; voxel resolution 47 × 47 × 1000 μm^3; spectral width of 100 kHz; echo delay time TE = 11.04 ms; recycle time TR = 1 s. Thus, all chemical shift selective images were T_1 and T_2 weighted in the same way. Selective radio frequency pulses (2000 Hz bandwidth, Gaussian shaped, truncated at 5% level) were used for slice selection.

The longitudinal magnetization decay (T_1) was measured by using the inversion−recovery sequence and the following parameters: inversion recovery time (2τ) from 100 μs to 20 s, NE = 50, and TR = 20 s. The transversal magnetization decay (T_2) was measured by using the common Hahn spin−echo technique using echo times ranging from 2 μs to 10 s, NE = 50, and TR = 20 s.

The heights of the peaks in the ^{1}H spectra versus the corresponding time, 2τ, were used to calculate the longitudinal and transversal relaxation values. The experimental data were fitted by the Maquardt−Levenberg algorithm, implemented by the Sigma Plot software (Jandel). Measurements were performed at the controlled temperature of 19 °C.

Chemical Analysis. *pH*. Five grams of sample was homogenized (Ultra-Turrax T25, IKA, Staufen, Germany) with 50 mL of distilled water and the pH measured using a pH-meter (model SA720, Orion Research, Boston, MA).

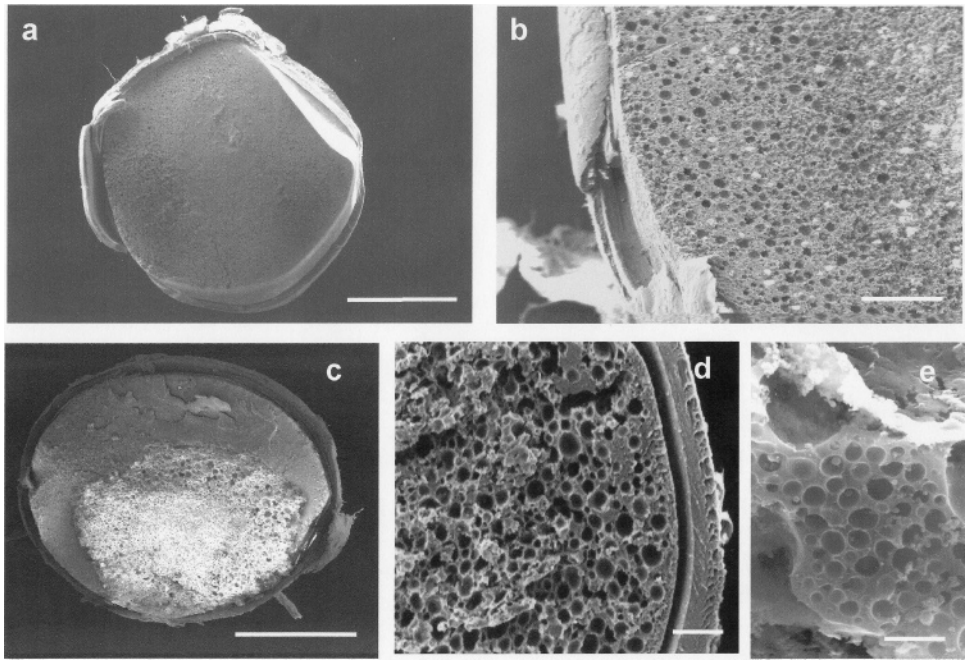

Figure 2. SEM images of eggs from white sturgeon (*A. transmontanus*). Fresh oocyte: (**a**) view of internal ultrastructure, scale bar = 1 mm; (**b**) cytoplasm encased by the multilayered coat, scale bar = 100 μm. Salted oocyte (caviar): (**c**) view of internal ultrastructure, scale bar = 1 mm; (**d**) cytoplasm encased by the multilayered coat, scale bar = 100 μm; (**e**) details of internal yolk nucleus, scale bar = 10 μm.

Proximate Composition. Each sample was assessed for moisture, protein (N × 6.25), fat, and sodium chloride content in accordance with AOAC (1990) methods (*18*).

Total volatile nitrogen (TVN) was determined as indicated in Pearson (*19*).

Fatty Acids. The extraction of total lipids was performed according to the method of Bligh and Dyer (*20*). For the preparation of fatty acid methyl esters the lipid sample (20 mg) was dissolved in 0.1 mL of tetrahydrofuran in a test tube, and 10% methanolic hydrogen chloride (2 mL) was added. A 0.1 mL solution of tricosanoic acid (10 mg mL^{-1}) was added as internal standard. The sample was sealed and heated at 100 °C for 1 h. To each sample was added 2 mL of a 1 M potassium carbonate solution. The fatty acid methyl esters were extracted with 2 × 2 mL of hexane, and 1 μL was injected into the gas chromatograph, in split mode (split ratio 1:50). Fatty acid analysis was carried out on a gas chromatograph (Agilent Technologies, model 6890 series) fitted with an automatic sampler (model 7683 series) and FID. The conditions used were the following: HP-Innowax fused silica capillary column (30 m × 0.25 mm i.d., 0.30 μm film thickness), temperature programmed from 150 to 180 °C at 3 °C min^{-1}, then from 180 to 250 °C at 2.5 °C min^{-1}, then held for 10 min. Carrier gas was helium at 1.0 mL min^{-1}, inlet pressure 16.9 psi. Fatty acids were identified relative to known external standards. The results are presented as grams per 100 g of fatty acids (percent by weight).

Data Analysis and Statistics. Chemical data were reported as mean values ± standard error of mean (SE). Homogeneity of variance was confirmed, and comparison between means was by one-way ANOVA. Student−Newman−Keuls was used as post hoc test for comparison of the means among different samplings. Significance was accepted at probabilities of ≤0.05. All of the statistical analyses were performed by SPSS 12.0 (SPSS Inc., Chicago, IL).

Both longitudinal and transversal water and lipid magnetization decays were fitted to a multiexponential function: the number of exponentials was correlated to the number of compartments where water (or lipids) was not in fast exchange. The set of the two-site exchange equations, first proposed by Hazelwood and co-workers (*21*) and described in ref *22*, was adopted for the data analysis.

Briefly, in a semilogaritmic plot of the magnetization decay [i.e., $\log(1 - M(t)/M_0)$] versus the delay time (2τ) between pulses, the least-squares linear regression analysis of the decay curve permits the resolution of the rate constant of the longer component. Subtraction of this component from the initial portion of the decay curve allows resolution of the rate constant of the faster component weighted by the number of protons, that is, the population fraction in each compartment.

Statistical analysis was performed on the T_1 and T_2 relaxation data calculated at the different times. The statistical significance of the differences was tested by comparing the slopes and the elevations of the fitted lines by means of the covariance analysis.

The experimental data were fitted by the Maquardt−Levenberg algorithm, implemented by the Sigma Plot software (Jandel). Statistical analysis was performed by the Prism program (version 4, GraphPad software).

RESULTS

SEM. The ultrastructure of fresh unsalted and NaCl-salted eggs of white sturgeon was studied using SEM. Eggs were spherical-shaped (≈2.5 mm in diameter) (**Figure 2a**,**c**) and encased in a multilayered envelope or chorion, ≈60 μm thick. The fresh egg, immature on the basis of size, seemed to be formed of material uniformly distributed (**Figure 2a**). The germinal vesicle and the animal pole/vegetal pole division were not emphasized with this technique. The yolk platelets, scattered in the whole cell (**Figure 2b**), were spherical with an average diameter of 35 μm.

The salted egg or caviar seemed to be constituted by two zones (**Figure 2c**): the first zone was formed by yolk platelets (**Figure 2d**) similar in size to the particles observed in the fresh egg, which occupied two-thirds of the cell and were concentrated at one of the hemispheres; the second zone, similar to a lunette, was constituted by very small spherical bodies, the volume of which was ≈180 μm^3 smaller than that of the yolk platelets. These particles were also present in the yolk (**Figure 2e**).

Chemical Analysis. As shown in **Table 1**, pH, TVN, moisture, and total protein and fat content values were collected on unsalted eggs at the isolation day and on salted eggs at different storage periods from 0 to 120 days. No significant variations were found in salted caviar during the entire storage period. The water content of unsalted samples was higher if compared to that of the salted samples. These differences are

Table 1. Chemical Parameters of Caviar from White Sturgeon (*A. transmontanus*) Unsalted (Raw) and Salted at Different Storage Periods (Mean ± SE)

	unsalted	salted				
		days of storage				
	raw	0	30	60	90	120
pH	6.10	6.15	6.16	6.20	6.20	6.22
moisture (%)	63.0 ± 0.36	58.2 ± 0.35	57.9 ± 0.47	57.6 ± 0.32	57.1 ± 0.20	56.8 ± 0.25
protein (%)	22.4 ± 0.13	23.9 ± 0.15	23.8 ± 0.00	23.7 ± 0.12	23.9 ± 0.20	24.0 ± 0.31
fat (%)	13.2 ± 0.08	14.5 ± 0.30	14.7 ± 0.17	14.6 ± 0.10	14.7 ± 0.12	14.9 ± 0.32
NaCl (%)	nd[a]	2.1 ± 0.05	2.1 ± 0.06	2.2 ± 0.08	2.3 ± 0.04	2.4 ± 0.12
TVN (mg of N/100 g)	20.2 ± 0.12	22.2 ± 0.12	22.4 ± 0.15	22.4 ± 0.12	22.4 ± 0.10	22.6 ± 0.18

[a] Not determined.

Table 2. Total Fatty Acid Composition of Caviar from White Sturgeon (*A. transmontanus*) Unsalted (Raw) and Salted at Different Storage Periods (Weight Percent, Mean ± SE)

	unsalted	salted				
		days of storage				
	raw	0	30	60	90	120
14:0	1.89 ± 0.03	2.00 ± 0.04	1.88 ± 0.01	2.04 ± 0.02	1.97 ± 0.18	1.98 ± 0.03
16:0	22.54 ± 0.22	22.81 ± 0.04	22.45 ± 0.11	22.04 ± 0.47	22.75 ± 0.35	22.79 ± 0.18
16:1n-7	4.68 ± 0.02	4.76 ± 0.02	4.72 ± 0.02	4.96 ± 0.07	4.75 ± 0.29	4.77 ± 0.03
18:0	2.89 ± 0.02	2.93 ± 0.01	3.03 ± 0.01	2.53 ± 0.21	3.03 ± 0.58	2.93 ± 0.07
18:1n-9	30.20 ± 0.04	30.51 ± 0.02	29.82 ± 0.14	30.96 ± 0.26	30.35 ± 1.24	30.18 ± 0.21
18:1n-7	3.19 ± 0.05	3.10 ± 0.06	3.38 ± 0.02	3.20 ± 0.06	3.07 ± 0.03	3.06 ± 0.03
18:2n-6	4.23 ± 0.05	4.34 ± 0.04	4.23 ± 0.02	4.51 ± 0.09	4.32 ± 0.24	4.30 ± 0.00
18:3n-6	0.61 ± 0.01	0.64 ± 0.01	0.62 ± 0.00	0.68 ± 0.02	0.63 ± 0.02	0.63 ± 0.00
18:3n-3	0.56 ± 0.02	0.60 ± 0.02	0.56 ± 0.00	0.62 ± 0.01	0.59 ± 0.01	0.59 ± 0.01
18:4n-3	0.57 ± 0.01	0.60 ± 0.01	0.61 ± 0.00	0.66 ± 0.00	0.65 ± 0.06	0.65 ± 0.02
20:1n-11	0.61 ± 0.01	0.64 ± 0.01	0.59 ± 0.00	0.66 ± 0.01	0.65 ± 0.59	0.64 ± 0.00
20:1n-9	1.76 ± 0.01	1.77 ± 0.00	1.75 ± 0.01	1.74 ± 0.03	1.82 ± 0.16	1.79 ± 0.00
20:2n-6	0.20 ± 0.11	0.23 ± 0.11	0.21 ± 0.11	0.22 ± 0.11	0.23 ± 0.11	0.23 ± 0.11
20:4n-6	2.06 ± 0.01	2.05 ± 0.01	2.21 ± 0.01	2.00 ± 0.02	2.11 ± 0.20	2.01 ± 0.08
20:5n-3 (EPA)	5.10 ± 0.05	5.08 ± 0.03	5.24 ± 0.03	4.89 ± 0.14	5.17 ± 0.42	5.12 ± 0.03
22:1n-11	0.21 ± 0.10	0.19 ± 0.10	0.19 ± 0.10	0.22 ± 0.11	0.00 ± 0.00	0.20 ± 0.10
22:1n-9	0.15 ± 0.07	0.14 ± 0.07	0.14 ± 0.07	0.18 ± 0.09	0.00 ± 0.00	0.15 ± 0.08
22:5n-3	1.25 ± 0.02	1.22 ± 0.02	1.23 ± 0.01	1.29 ± 0.02	1.25 ± 0.01	1.24 ± 0.01
22:6n-3 (DHA)	16.97 ± 0.24	16.12 ± 0.50	16.74 ± 0.08	16.29 ± 0.16	16.49 ± 0.67	16.46 ± 0.11
24:1n-9	0.31 ± 0.18	0.27 ± 0.13	0.34 ± 0.17	0.24 ± 0.12	0.18 ± 0.09	0.29 ± 0.15
total SFA	27.32 ± 0.15	27.74 ± 0.09	27.35 ± 0.13	26.61 ± 0.66	27.75 ± 0.04	27.69 ± 0.27
total MUFA	41.11 ± 0.34	41.39 ± 0.29	40.93 ± 0.14	42.17 ± 0.69	40.82 ± 0.89	41.08 ± 0.06
total PUFA	31.56 ± 0.27	30.87 ± 0.38	31.71 ± 0.01	31.22 ± 0.02	31.43 ± 0.85	31.22 ± 0.22
total n-3	23.21 ± 0.48	22.40 ± 0.52	23.14 ± 1.00	22.46 ± 0.28	22.89 ± 0.01	22.81 ± 1.18
total n-6	8.15 ± 0.71	8.25 ± 0.90	8.29 ± 1.01	8.47 ± 0.11	8.31 ± 0.86	8.18 ± 0.96
n-6/n-3	0.35 ± 0.42	0.37 ± 0.48	0.36 ± 0.60	0.38 ± 0.07	0.36 ± 0.41	0.36 ± 0.59

probably caused by salt content, which leads to increased dehydration of eggs. As a consequence, the mass balance for the other components is biased on the differences in water content.

The total fatty acid composition of salted caviar at different times of storage is presented in **Table 2**. The dominant saturated fatty acid (SFA) in caviar was palmitic acid (16:0) and contributed >80% to the saturated fatty acids. Other saturated fatty acids were myristic (14:0) and stearic (18:0) acids. The amount of monounsaturated fatty acids (MUFA) was ≈41%, oleic acid (18:1n-9) being the most representative. Other monoenes were 18:1n-7 (3%), 20:1n-9 (1.8%), and 20:1n-11 (0.6%). The percentage of polyunsaturated fatty acids (PUFA) in caviar was 31−32%. Among the n-6 fatty acids the amounts of 18:2n-6 and its metabolic product 20:4n-6 were 4.2 and 2.1%, respectively. With regard to the n-3 series, 22:6n-3 (docosahexaenoic acid, DHA) and 20:5n-3 (eicosapentaenoic acid, EPA) were dominant, with percentages of 16−17 and 5%, respectively. They contributed >70% to the total n-3 fatty acids in caviar. In all samples the amount of n-3 PUFAs was 3 times higher than the n-6 PUFAs, with a n-6/n-3 ratio of ≈0.35.

The fatty acid composition of caviar from farmed *A. transmontanus* appeared to be similar to those published by other authors for farmed *Acipenser baeri*, *A. transmontanus*, and *Polyodon spathula* and for wild *Huso huso*, *Acipenser gueldenstaedtii*, *A. transmontanus*, *Acipenser fulvescens*, and *Acipenser stellatus* (*16*, *17*, *23*). If compared with caviar from other wild sturgeons, the caviar from cultured *A. transmontanus* was characterized by a higher level of 18:2n-6 and a lower level of 20:4n-6. This was probably due, as well-known from the literature, to the different diets, in particular to the effect of vegetable oil contained in the commercial feed. When the fatty acid compositions of caviar were compared at 0, 30, 60, 90, and 120 days of storage at 4 °C, no significant differences were found. As evidenced in **Tables 1** and **2**, the chemical composition of salted caviar was practically constant over the entire storage period.

NMR Measurements. *^{1}H T_1 and T_2 Relaxation Parameters.* T_1 relaxation decay of lipid components was found to be biexponential in both unsalted and salted eggs. **Table 3** shows the T_1 values of short and long components as obtained on unsalted and salted caviar samples at 0 days and after 60

Table 3. ^{1}H T_1 and T_2 Relaxation Times of Lipid Components and Population Fraction Percentages of Caviar from White Sturgeon (*A. transmontanus*)[a]

		unsalted		salted	
		0 days	60 days	0 days	60 days
T_1 (ms)	short	371 ± 2.6	643 ± 10.9	383 ± 26.5	478 ± 7.6
population fraction (%)		78	82	88	85
T_1 (ms)	long	805 ± 27.1	1780 ± 67.4	928 ± 63.1	1555 ± 80.3
population fraction (%)		22 ± 0.3	28 ± 4.3	12 ± 1.5	15 ± 0.9
T_2 (ms)		46 ± 0.5	46 ± 0.8	51 ± 0.2	51 ± 0.3
population fraction (%)		98 ± 0.2	98 ± 0.4	98 ± 0.1	98 ± 0.6

[a] Standard deviations are reported. R^2 correlation values were in the range of 0.98–0.99.

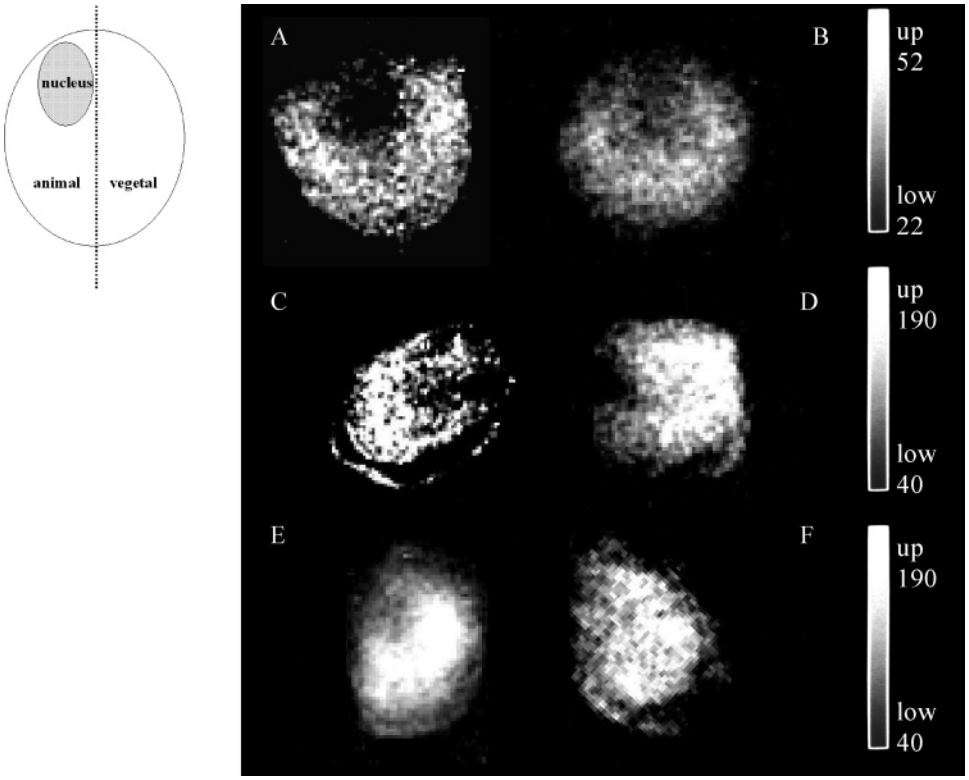

Figure 3. NMR images selective on lipids of eggs from white sturgeon (*A. transmontanus*): fresh oocytes at (**A**) 0 days and (**B**) 60 days; salted oocytes at (**C**) 0 days, (**D**) 60 days, (**E**) 90 days, and (**F**) 120 days. Voxel resolution: $47 \times 47 \times 1000$ μm^3. On the left side is shown a scheme of the egg with animal and vegetal pole division.

days of storage, together with relative population fractions of the two components (percent). In particular, it can be observed that at 0 days T_1 values of each component were quite similar in unsalted (long, 805 ms; short, 371 ms) and salted (long, 928 ms; short, 383 ms) eggs. At 60 days of storage both components of unsalted (long, 1780 ms; short, 643 ms) and salted (long, 1555 ms; short, 478 ms) eggs significantly lengthened ($P < 0.0001$), whereas the relative populations slightly increased.

By means of the two-site exchange model, the short component of the T_2 relaxation decay was much more populated (98%) than the long one in both kinds of samples. T_2 values of unsalted (46 ms) and salted (51 ms) eggs were found to be similar, and during storage they did not change significantly.

MRI. **Figure 3** shows lipid selective images collected on both unsalted and salted eggs at the day of isolation (**Figure 3A**,**C**) and after 60 days of storage (**Figure 3B**,**D**). In the unsalted egg, at 0 days (**Figure 3A**), lipids are present only in the vegetal pole, showing low signal intensity. By contrast, in the salted sample (**Figure 3C**) lipids are more uniformly distributed in the cell without compartmentalization, except for the empty space at the periphery of the cell.

After 60 days of storage (**Figure 3B**), the image contrast of the unsalted egg showed that lipids were still mainly localized in the vegetal pole and only partially in the animal pole, but with a signal intensity significantly increased. After the same 60 days of storage, the image contrast of salted samples (**Figure 3D**) indicated that lipids had already invaded the animal pole, showing a highly increased signal intensity. Panels **E** and **F** of **Figure 3** show lipid-selective SE images of salted samples at 90 and 120 days, respectively. In these images, lipids appear to be mostly uniformly distributed in the cell, showing a high signal intensity.

DISCUSSION

Caviar is composed by the unfertilized eggs of female sturgeons. The sturgeon egg is polar, showing an animal and a vegetal pole (*24*, *25*). Oocyte maturity can be identified by the position of the egg nucleus, called the germinal vesicle (GV).

Table 4. ^{1}H T_1 and T_2 Relaxation Times of Lipid Components of Eggs from White Sturgeon (*A. transmontanus*) and *X. laevis*

reference	this paper	Paüser et al. (*30*)	Cameron et al. (*31*)	Sehy et al. (*32*)	Sehy et al. (*32*)
T_1 (ms)	371	459	443	380	390 (animal) 450 (vegetal)
T_2 (ms)	46	24.44		25	27 (animal) 25 (vegetal)
oocyte species	white sturgeon	*X. laevis*	*X. laevis*	*X. laevis*	*X. laevis*
field (tesla)	4.7	>4.7	<4.7	4.7 spectroscopic	4.7 localized

In immature oocytes (early vitellogenesis), the GV occupies a central position but migrates toward the egg periphery as development proceeds. When the GV nears the animal pole, the oocytes are mature (late vitellogenesis) (*26*).

During maturation of the amphibian oocyte (*27*), the cytoplasm is involved in the elaboration of organelles, ground substance, and inclusion bodies such as yolk platelets. All of these inclusions are essential for future growth and differentiation, because they serve both as a potential source of energy and as a reservoir of metabolites. The developing amphibian oocyte is characterized by an enormous increase in the yolk deposition in all of the cytoplasm. In sturgeon oocytes, the yolk bodies first appear in the peripheral cytoplasm and, as maturation proceeds, exhibit centripetal progression similar to yolk deposition in the amphibian oocyte (*28*, *29*). There are three forms of yolk: carbohydrate, fatty, and protein yolk. Gradually, the yolk platelets and the lipid-containing bodies (known as lipochondria) are distributed in the entire cytoplasm.

When the GV migrates to the animal hemisphere, the large yolk bodies and oil droplets aggregate in the vegetal pole (*26*). As reported, in caviar, the dominant fatty acid is oleic acid (in the range of 32.9−42.9%), which has been found to be the main source of energy during embryological development together with high amounts of polyunsatured fatty acids (*16*).

Lipids are localized in the cytoplasm mainly in the vegetal pole, whereas they are absent or in poor amount in the nucleus. Accordingly, lipid-selective MRI images of caviar showed that almost no lipids were present in the nucleus. As for the relaxation parameters, it is worth comparing T_1 and T_2 lipid relaxations previously characterized in *Xenopus* oocytes by many investigators, both on a single large lipid resonance (*30*, *31*) or by resolving all lipid resonances (*32*). Interestingly, no authors reported a biexponential model for describing the T_1 relaxation rate. As shown in **Table 4**, Paüser (*30*) reported a T_1 of 459 ms as measured (at 7 T) on a single large resonance; Cameron (*31*) calculated a T_1 of 443 ms on the major lipid peak at ≈1.8 ppm, and Sehy (*32*) reported four values for T_1 as calculated on the four lipid signals at 5.2, 2.7, 1.9, and 1.2 ppm, namely, 680, 490, 380, and 390 ms, respectively (at 4.7 T). Therefore, the value of 371 ms calculated in the present paper for the short component of T_1 in the unsalted oocytes of *A. transmontanus* is in good agreement with previous values. Moreover, relaxation parameters, mainly representative of the vegetal pole characteristics (yolk platelet distribution, microtubules, tubulin, and actin subunit pools) indicated that in unsalted oocytes the distribution of short and long components was highly shifted toward immobilized lipids (T_1 short ≈80%; T_2 short ≈100%) according to their localization in yolk platelets.

Again, by comparing the T_2 values calculated for *Xenopus* oocytes, Paüser (*30*) reported a T_2 of 24.44 ms, as measured on a single large resonance, and Sehy (*32*) calculated four values, 25, 28, 25, and 30 ms, for the four resolved lipid signals. Hence, the T_2 short component of 46 ms calculated in the present paper for *A. transmontanus* is quite longer. During a 60-day storage, both short and long components of T_1 significantly lengthened (≈200%): during the same time the oocyte became mushy, indicating that denaturation was occurring. The lengthening of T_1 suggests that the aging process could activate the hydrolysis of lipids, making them much more mobile. On the contrary, during the same storage period the T_2 value did not change at all, preventing any possible correlation with the T_1 trend.

In salted samples at 0 days, short and long T_1 values were found to be unchanged relative to the unsalted oocytes, the short component still being the most populated. This finding seems to suggest that the osmotic effect produced by salting has practically no effect on lipids, at short times. Accordingly, SEM analysis did not find significant alterations upon the salting procedure. During the 60-day storage, both short and long components of T_1 lengthened, but to a minor degree (around 150%) compared to the unsalted oocytes.

In salted eggs the T_2 value was kept almost invariant during the entire period of storage. This invariance observed both in salted and in unsalted eggs might be correlated to the combination of two different opposite events: the higher mobility of lipid components most likely deriving from lipolysis and the cell shrinkage due to osmotic processes and water evaporation, which make the cytoplasm structure more rigid (*22*).

In unsalted caviar eggs the NMR image selective on lipids appeared to be quite similar to those reported in the literature for *Xenopus* oocytes: lipid distribution in the cell showed a very weak signal from the nucleus (6 times lower than the signal from the cytoplasm), whereas most lipids were found in the cytoplasm. NMR images of *Xenopus* oocytes first reported by Aguayo et al. (*33*) showed a significant contrast between intracellular regions that the authors ascribed to a strong chemical shift artifact deriving from cytoplasmic lipids.

Posse and Aue (*34*), using a 4D spectroscopic imaging technique, localized the lipid resonance into the cytoplasm, as well. More recently, by using spin density-weighted images, specific on lipids, Sehy (*32*) found that lipid was decreasing from vegetal to animal pole.

In the image of *A. transmontanus* unsalted egg at 0 days, lipids are present only in the vegetal pole (**Figure 3A**), showing low signal intensity, thus suggesting a high immobilization as expected for lipids localized in a highly heterogeneous structure.

After 60 days of storage (**Figure 3B**), the image contrast of the unsalted egg showed that lipids were still localized in the vegetal pole. However, the signal intensity was found to be significantly increased, thus indicating a much higher mobility.

Differently from the unsalted caviar, salted samples exhibited an almost uniform distribution of lipids in the cell, without compartmentalization, right from the 0 day (**Figure 3C**). After 60 days of storage (**Figure 3D**), the image contrast indicated that lipids had already invaded part of the animal pole, showing highly increased signal intensity, hence suggesting that lipids had become more mobile. After longer storage periods (90 and 120 days, **Figure 3E**,**F**, respectively), lipids appeared to be mostly uniformly distributed in the cell and endowed with a great mobility.

In conclusion, MRI results well validated the relaxation spectroscopic data according to which lipids were found to be endowed with two different mobility regimes, one slow (short T_1) and one fast (long T_1), both lengthening with storage time. This finding suggests that during a long storage period of up to ≈120 days at 4 °C, lipid hydrolysis is still strongly active in salted eggs and gives rise to much more mobile fragments, responsible for both higher contrast in the lipid images and lengthening in the relaxation parameters. Chemical analysis performed on salted samples stored at 4 °C for the same period assessed a total fat content of 13.8% that remained practically unchanged and a constant fatty acid composition. Therefore, by combining chemical and NMR results it is possible to (a) suppose that a mechanism of lipid hydrolysis (faster in unsalted than in salted eggs) is still occurring during the storage of caviar at 4 °C up to ≈4 months and (b) exclude that an intensive oxidative process is active in the same storage period.

Stodolnik et al. (*35*) as well hypothesized that a salt content of 2.3−7.0% did not stop the proteolytic enzyme activity in sea trout eggs. Interestingly, when fish tissues instead of eggs were investigated, a lowering of the total lipid values was observed in three lipid tissues of a commercial sturgeon hybrid, *Acipenser baeri* × *A. transmontanus*, stored at 4 °C for a period of 5 days (*36*) and attributed to the oxidative process of the lipid matter preceded by a strong activity of hydrolytic enzymes. Oxidative changes of lipids during fish canning, in particular tuna samples and salmon white muscle, were reported as well (*37*). In conclusion, on the basis of data collected in this study, we suggest that the lipoprotein hydrolysis process, in fish as in avian eggs (*38*) and much more efficiently than in tissues, might develop active components endowed with antimicrobial properties able to prevent fast egg degradation.

ACKNOWLEDGMENT

We are grateful to Dr. Filippo Vaini for practical assistance, to Agroittica Lombarda (Calvisano, BS, Italy) for providing caviar samples, and to Giulio Zannoni for helpful technical assistance.

LITERATURE CITED

(1) Givens, D. I.; Frayn, K. N. Fat in the diets of animal and man. *Br. J. Nutr.* **1997**, *78* (Suppl. 1).

(2) Fitzgerald, G. A. Omega 3 fatty acids and vascular function. *Omega-3 News* **1993**, *9*, 1−3.

(3) AA.VV. *1998: The Return of ω-3 Fatty Acids into Food Supply. 1. Land Based Animal Food Products and Their Health Effects*; Kargel AG and B. A. Linke: Basel, Switzerland, 1998; XII, pp 240.

(4) Brady, D.; Gaines, S.; Fenelon, L.; McPartlin, J.; O'Farrelly, C. A. Lipoprotein-derived antimicrobial factor from hen-egg yolk is active against *Streptococcus* species. *J. Food Sci.* **2002**, *67*, 3096−3103.

(5) Brady, D.; Lowe, N.; Gaines, S.; Fenelon, L.; McPartlin, J.; O'Farrelly, C. Inhibition of *Streptococcus mutans* growth by hen egg-derived fatty acids. *J. Food Sci.* **2003**, *68*, 1433−1437.

(6) Bourgeois, C.; Givens, D. I.; Frayn, K. N.; Hiraoka, A.; Naruse, U. L'evolution physico-chimique et la maturation de la viande et de la chair de poisson. *ADRIA* **1974**, *2*.

(7) Merkel, J. R.; Dreisbach, J. H.; Ziegler, H. B. Collagenolitic activity of some marine bacteria. *Appl. Environ. Microbiol.* **1975**, *29*, 145−151.

(8) Hiraoka, A.; Naruse, U. Effect of starvation on fatty acid composition of farmed sturgeon Ext. Abs., Aquaculture Tech. Prod. Systems. *J. Appl. Ichtyol.* **1999**, *15*, 327.

(9) Hardy, R.; Keay, J. N. Seasonal variation in the chemical composition of Cornish mackerel *Sgomber scombrus* (L) with detailed references to the lipids. *J. Food Technol.* **1972**, *7*, 125−127.

(10) Ke, P. J. Differential lipid oxidation in various parts of frozen mackerel. *J. Food Technol.* **1977**, *12*, 37−47.

(11) Ackman, R. G.; Eaton, C. A.; Linke, B. A. Differentiation of freshwater characteristics of fatty acids in marine specimens of the Atlantic sturgeon *Acipenser oxyrhynchus*. *Fish. Bull.* **1972**, *73*, 838−845.

(12) Valin, C. Charactéristiques qualitatives et technologiques des viandes bovines: influence des conditions d'abatage et de la technologie. In *Production de Viande Bovine*; INRA: Paris, France, 1986; pp 85−98.

(13) Laghi, L.; Cremonini, M. A.; Placucci, G.; Sykora, S.; Wright, K.; Hills, B. A proton NMR relaxation study of hen egg quality. *Magn. Reson. Imaging* **2005**, *23*, 501−510.

(14) Linares-Casenave, J.; Van Eenennaam, J. P.; Doroshov, S. I. Ultrastructural and histological observations on temperature-induced follicular ovarian atresia in the white sturgeon. *J Appl. Ichthyol.* **2002**, *18*, 382−390.

(15) Congiu, L.; Fontana, F.; Patarnello, T.; Rossi, R.; Zane, L. The use of AFLP in sturgeon identification. *J Appl. Ichthyol.* **2002**, *18*, 286−289.

(16) Wirth, M.; Kirschbaum, F.; Gessner, J.; Krüger, A.; Patriche, N.; Billard, R. Chemical and biochemical composition of caviar from different sturgeon species and origin. *Nahrung* **2000**, *44*, 233−237.

(17) Gessner, J.; Wirth, M.; Kirshbaum, F.; Krüger, A.; Patriche, N. Caviar composition in wild and cultured sturgeons—impact of food sources on fatty acid composition and contaminants load. *J. Appl. Ichthyol* **2002**, *18*, 665−672.

(18) AOAC. In *Official Methods of Analysis*, 15th ed.; Association of Official Analytical Chemists: Arlington, VA, 1990.

(19) Pearson, D. *Laboratory Techniques in Food Analysis*, 1st ed.; Butterworth: London, U.K., 1973.

(20) Bligh, E. G.; Dyer, W. J. A rapid method of total lipid extraction and purification. *Can. J. Biochem. Physiol.* **1959**, *37*, 911−917.

(21) Hazelwood, C. F.; Chang, D. C.; Nichols, B. L.; Woessner, D. E. Nuclear magnetic resonance transverse relaxation times of water protons in skeletal muscle. *Biophys. J.* **1974**, *14*, 583−606.

(22) Gussoni, M.; Greco, F.; Vezzoli, A.; Paleari, M. A.; Moretti, V. M.; Lanza, B.; Zetta, L. Osmotic and aging effects in caviar oocytes throughout water and lipid changes assessed by ^{1}H NMR T_1 and T_2 relaxation and MRI. *Magn. Reson. Imaging* **2006**, submitted for publication.

(23) Czesny, S.; Dabrowski, K.; Christensen, J. E.; Van Eenennaam, J.; Doroshov, S. Discrimination of wild and domestic origin of sturgeon ova based on lipids and fatty acid analysis. *Aquaculture* **2000**, *189*, 145−153.

(24) Cherr, C. N.; Clark, W. H., Jr. Fine structure of the envelope and micropyles in the eggs of the white sturgeon, *Acipenser transmontanus* Richardson. *Dev., Growth Differ.* **1982**, *24*, 341−352.

(25) Cherr, C. N.; Clark, W. H., Jr. Gamete interaction in the white sturgeon *Acipenser transmontanus*: a morphological and physiological review. *Environ. Biol. Fishes* **1985**, *14*, 11−22.

(26) Linares-Casenave, J.; Kroll, K. J.; Van Eenennaam, J. P.; Doroshov, S. I. Effect of ovarian stage on plasma vitellogenin and calcium in cultured white sturgeon. *Aquaculture* **2003**, *221*, 645−656.

(27) Wischnitzer, S. The ultrastructure of the cytoplasm of the developing amphibian egg. *Adv. Morphog.* **1966**, *5*, 131−179.

(28) Raikova, E. V. Ultrastructure of sterlet (*Acipenser ruthenus*) oocytes during early vitellogenesis. II Cytoplasmic fine structure. *Tsitologiia* **1974**, *16*, 679−684.

(29) Doroshov, S. I.; Moberg, G. P.; Van Eenennaam, J. P. Observations on the reproductive cycle of cultured white sturgeon, *Acipenser transmontanus*. *Environ. Biol. Fishes* **1997**, *48*, 265−278.

(30) Paüser, S.; Zschunke, A.; Khuen, A.; Keller, K. Estimation of water content and water mobility in the nucleus and cytoplasm of *Xenopus laevis* oocytes by NMR microscopy. *Magn. Reson. Imaging* **1995**, *13*, 269−276.

(31) Cameron, I. L.; Merta, P.; Fullerton, G. D. Osmotic and motional properties of intracellular water as influenced by osmotic swelling and shrinkage of *Xenopus* oocytes. *J. Cell Physiol.* **1990**, *142*, 592−602.
(32) Sehy, J. V.; Ackerman, J. J. H.; Neil, J. J. Water and lipid MRI of the *Xenopus* oocyte. *Magn. Reson. Med.* **2001**, *46*, 900−906.
(33) Aguayo, J. B.; Blackband, S. J.; Schoeniger, J.; Mattingly, M. A.; Hintermann, M. Nuclear magnetic resonance imaging of a single cell. *Nature* **1986**, *322*, 190−191.
(34) Posse, S.; Aue, W. P. Spectroscopic imaging and gradient-echo microscopy on a single cell. *J. Magn. Reson.* **1989**, *83*, 620−625.
(35) Stodolnik, L.; Salacki, M.; Rogozinska, E. Effects of sea trout egg quality on stability of salted roe during cold-storage. *Nahrung* **1992**, *36*, 325−332.
(36) Berni, P.; Mele, P.; Serra, L. A.; Cararosa, L.; Secchiari, P. Monitoring of fatty acid composition of intraperitoneal, subcutaneous and intramuscular fat in commercial hybrids of sturgeon (*Acipenser baeri* × *Acipenser transmontanus*) during storage at 4 °C. *Int. Rev. Hydrobiol.* **2002**, *87*, 613−620.
(37) Medina, I.; Sacchi, R.; Giudicianni, I.; Aubourg, S. Oxidation in fish lipids during thermal stress as studied by C-13 nuclear magnetic resonance spectroscopy. *J. Am. Oil Chem. Soc.* **1998**, *75*, 147−154.
(38) Kovacs-Nolan, J.; Phillips, M.; Mine, Y. Advances in the value of eggs and egg components for human health. *J. Agric. Food Chem.* **2005**, *53*, 8421−8431.

Received for review May 8, 2006. Revised manuscript received June 22, 2006. Accepted June 29, 2006.

JF061286F